Remote Sensing of Environment 236 (2020) 111501

Contents lists available at ScienceDirect

Remote Sensing of Environment

journal homepage: www.elsevier.com/locate/rse

Modelling above-ground biomass stock over Norway using national forest inventory data with ArcticDEM and Sentinel-2 data

S. Puliti[a,*], M. Hauglin[a], J. Breidenbach[a], P. Montesano[b,c], C.S.R. Neigh[c], J. Rahlf[a], S. Solberg[a], T.F. Klingenberg[d], R. Astrup[a]

[a] Norwegian Institute for Bioeconomy Research (NIBIO), Division of Forest and Forest Resources, National Forest Inventory, Høgskoleveien 8, 1433 Ås, Norway
[b] Science Systems and Applications, Inc., 10210 Greenbelt Road, Lanham, MD, 20706, USA
[c] Biospheric Sciences Laboratory, Code 618 NASA Goddard Space Flight Center, Greenbelt, MD, 20771, USA
[d] Norwegian Mapping Authority (Kartverket), Land Mapping Division, P.O. Box 600, Sentrum, 3507, Hønefoss, Norway

ARTICLE INFO

Keywords:
Space-borne imagery
Stereogrammetry
Boreal forest structure
Biomass mapping
Open data

ABSTRACT

Boreal forests constitute a large portion of the global forest area, yet they are undersampled through field surveys, and only a few remotely sensed data sources provide structural information wall-to-wall throughout the boreal domain. ArcticDEM is a collection of high-resolution (2 m) space-borne stereogrammetric digital surface models (DSM) covering the entire land area north of 60° of latitude. The free-availability of ArcticDEM data offers new possibilities for aboveground biomass mapping (AGB) across boreal forests, and thus it is necessary to evaluate the potential for these data to map AGB over alternative open-data sources (i.e., Sentinel-2). This study was performed over the entire land area of Norway north of 60° of latitude, and the Norwegian national forest inventory (NFI) was used as a source of field data composed of accurately geolocated field plots ($n = 7710$) systematically distributed across the study area. Separate random forest models were fitted using NFI data, and corresponding remotely sensed data consisting of either: i) a canopy height model (ArcticCHM) obtained by subtracting a high-quality digital terrain model (DTM) from the ArcticDEM DSM height values, ii) Sentinel-2 (S2), or iii) a combination of the two (ArcticCHM + S2).

Furthermore, we assessed the effect of the forest- and terrain-specific factors on the models' predictive accuracy. The best model (,i.e., ArcticCHM + S2) explained nearly 60% of the variance of the training set, which translated in the largest accuracy in terms of root mean square error (RMSE = 41.4 t ha^{-1}). This result highlights the synergy between 3D and multispectral data in AGB modelling.

Furthermore, this study showed that despite the importance of ArcticCHM variables, the S2 model performed slightly better than ArcticCHM model. This finding highlights some of the limitations of ArcticDEM, which, despite the unprecedented spatial resolution, is highly heterogeneous due to the blending of multiple acquisitions across different years and seasons. We found that both forest- and terrain-specific characteristics affected the uncertainty of the ArcticCHM + S2 model and concluded that the combined use of ArcticCHM and Sentinel-2 represents a viable solution for AGB mapping across boreal forests. The synergy between the two data sources allowed for a reduction of the saturation effects typical of multispectral data while ensuring the spatial consistency in the output predictions due to the removal of artifacts and data voids present in ArcticCHM data. While the main contribution of this study is to provide the first evidence of the best-case-scenario (i.e., availability of accurate terrain models) that ArcticDEM data can provide for large-scale AGB modelling, it remains critically important for other studies to investigate how ArcticDEM may be used in areas where no DTMs are available as is the case for large portions of the boreal zone.

1. Introduction

Stereogrammetric data generated by matching stereo pairs of high-resolution space-borne imagery (HRSI) have been used for nearly 15 years to map forest canopy height and above-ground biomass (AGB) stocks (Poon et al., 2005; St-Onge et al., 2008). Despite the advantage of providing finely detailed information on the forest canopy structure over vast areas (from 100 up to millions of km^2), their use in the

* Corresponding author.
E-mail address: stefano.puliti@nibio.no (S. Puliti).

https://doi.org/10.1016/j.rse.2019.111501
Received 18 June 2019; Received in revised form 11 October 2019; Accepted 26 October 2019
Available online 07 November 2019

scientific literature has been limited compared to other space-borne medium resolution multispectral imagery.

The recently released and freely available ArcticDEM (arcticdem.org) digital surface model (DSM) data set is a collection of HRSI stereogrammetric data covering the entire hemiboreal zone (just over 10% of the planet) (Porter et al., 2018). The ArcticDEM offers unprecedented opportunities to map and estimate the forest attributes in the circumboreal region (Meddens et al., 2018). Meddens et al. (2018) and Montesano et al. (2017, 2019) demonstrated that DSMs from HRSI data could be used to map canopy height. However, the potential for using the ArcticDEM for large scale mapping of AGB stocks in boreal forests, to our knowledge, has not been investigated at a national or regional scale. Currently, much of the large-scale remote sensing-based efforts on forest AGB mapping are targeted at the tropics (e.g., GEDI mission). Nevertheless, boreal forests cover approximately 9.2 million km^2 (29% of the global forest area), and they represent approximately 20% of the total forest carbon sink (Pan et al., 2011) and one of the major carbon pools of living organic carbon on Earth (Kuusela, 1990). The current study represents the first effort to utilize ArcticDEM data at a national scale to model AGB in Norwegian boreal forests using ground reference data from the Norwegian National Forest Inventory (NFI).

Modelling and mapping of forest AGB with HRSI stereogrammetric data have been demonstrated for Forest Management Inventory (FMI) over relatively small areas (9–300 km^2) (St-Onge et al., 2008; Persson et al., 2013; Straub et al., 2013; Persson, 2016; Persson and Perko, 2016; Fassnacht et al., 2017; Pearse et al., 2018; Vastaranta et al., 2018). For the FMI focused studies, the HRSI data were acquired on-demand, and often fine geometric adjustments were performed to reduce the geometric errors in the HRSI DEMs. The results of these studies performed in "controlled" environments were encouraging, revealing AGB models with adjusted R^2s and root mean square errors (RMSEs) in the ranges 0.43–0.79 and 32–70 t ha^{-1} (20%–46%). Nevertheless, these results may not be representative of large-scale data such as the ArcticDEM which are the result of multiple HRSI acquisitions under different acquisition geometry (i.e., the combination of sun angle and viewing angle), atmospheric, and seasonal conditions. Furthermore, in contrast to previous studies done in an FMI context, the geometric corrections performed on the ArcticDEM data are done using sparse samples of the Geoscience Laser Altimeter System (GLAS) pulses. To date, most studies focused on forest management inventories and only in a few examples HRSI data were used in the context of large-scale forest mapping (Immitzer et al., 2016; Neigh et al., 2016; Montesano et al. 2017, 2019; Meddens et al., 2018). Only in Germany was, NFI data used as ground truth (Immitzer et al., 2016), and where results were promising showing growing stock predictions with a root mean square error of 32% of the mean. The German study was performed using two WorldView-2 stereo-pairs acquired within a few minutes and the accuracy found by Immitzer et al. (2016) is hardly representative of the hundreds of thousands of scenes used in ArcticDEM. The pre-requirement for all of the abovementioned studies was that a digital terrain model (DTM) was available to normalize the HRSI DSM or to subtract the terrain height from the HRSI DSM height above the ellipsoid to generate a canopy height model (CHM) in meters above-ground. While such a prerequisite may limit the applicability of HRSI stereogrammetric data, in some cases accurate DTMs are freely accessible for entire countries (e.g., Norway). The evaluation of ArcticDEM data under the best-case scenario where a DTM is available wall-to-wall, thus enabling the evaluation of the full potential of ArcticDEM data for AGB modelling. Henceforth, the term ArcticCHM will be used to refer to the height-normalized ArcticDEM data.

The factors affecting the quality of the HRSI DSMs and the potential for modelling canopy height using ArcticDEM data (i.e., without the need of an accurate DTM) are starting to be understood thanks to the studies by Montesano et al. (2017); Montesano et al. (2019) and Meddens et al. (2018). Amongst these, Montesano et al. (2017, 2019) highlighted the seasonal variations and varying sun-target-sensor geometry as some of the critical factors affecting the quality of the DSMs for different forest types. The considerable variations in seasonal and sun-target-sensor geometry amongst different ArcticDEM acquisitions may limit its use for wall-to-wall AGB mapping. Despite the pioneering role of the abovementioned studies, they were limited by lack of in-situ observations, and thus the accuracy of canopy height measures from the HRSI DSM was limited to comparison to samples of airborne laser scanner (ALS) DSMs or small amounts of spatially limited field plots. In order to utilize ArcticDEM data for large-scale circumboreal forest AGB assessment, it is critical to gain a better understanding of the quality of the models linking ArcticDEM data with ground reference AGB over large areas and based on large numbers of stereo image-pairs.

The literature highlights that there is a synergy between using the DEM in combination with spectral information from HRSI stereogrammetric data for mapping forest attributes (Wallerman et al., 2010; Persson et al., 2013; Kattenborn et al., 2015; Immitzer et al., 2016; Persson, 2016; Fassnacht et al., 2017; Meddens et al., 2018). A common finding is that the inclusion of multi-spectral information improved the models' predictive ability. As an example, Fassnacht et al. (2017) found that the spectral variables differentiating coniferous and deciduous tree species had a higher explanatory power for AGB than height-related variables. Concerning the spectral data, ArcticDEM data only includes the DEM and not the original imagery used for the DEM production. However, several medium-resolution (10–30 m) space-borne multi-spectral data are available free of charge (e.g., Sentinel-2 or Landsat 8 data), and these data sources can be combined with the height information from the ArcticDEM.

The objective of this study was to model AGB for all of Norway at latitudes north of 60° using Norwegian NFI data, ArcticDEM data, and Sentinel-2 data. This study, to our knowledge, is the first to utilize large-scale HRSI stereogrammetric data in combination with an extensive network of ground reference observations.

2. Materials and methods

2.1. Study area

The study area was the land area of Norway at latitudes north of 60° (260 000 km^2). Approximately 34% of this study area was estimated to be forested, all of which was classified as boreal coniferous forest (NIBIO, 2015). The main tree species in the study area were Norway spruce (*Picea abies* (L.) Karst.), Scots pine (*Pinus sylvestris* L.), and birch (*Betula pubescens*) (NIBIO, 2015).

2.2. National forest inventory data

The Norwegian NFI (Tomter et al., 2010) was used as ground reference data. The NFI consisted of permanent sample plots located across the country according to a stratified systematic design. The stratification was based on the forest productivity, with a grid spacing of 3 km × 3 km, 3 km × 9 km, and 9 km × 9 km for productive, mountainous, and mountainous forests in northern Norway (Finnmark county). Each plot is re-measured every five years, and as such, 20% of the total number of plots are measured every year as a part of an interpenetrating panel design.

The NFI plots were circular with an area of 250 m^2. Within each plot, all trees with a diameter at breast height (DBH) ≥ 5 cm were calipered, while height was measured for a sample of ten trees selected according to probability proportional to stem basal area. The height of every tree was measured on plots with less than ten trees. For the trees with no height measurement, height was predicted using DBH-height models calibrated with plot-level measurements. Single-tree AGB was predicted for each tree using species-specific allometric models by Marklund (1988) using DBH and tree height. The plots' AGB was the sum of the trees' AGB scaled to per hectare values. Dominant tree

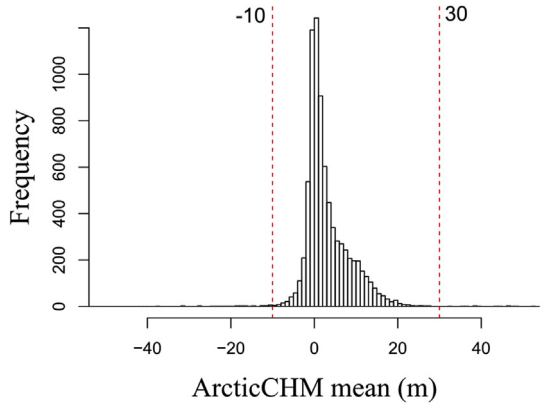

Fig. 1. Distribution of ArcticCHM mean height for the reduced set of NFI plots ($n=$ 8431). The red dashed lines represent the thresholds −10 m and 30 m used to define the reliability of ArcticCHM data. (For interpretation of the references to color in this figure legend, the reader is referred to the Web version of this article.)

species were allocated to three classes (spruce, pine, or deciduous species) according to the species with the largest proportion of AGB in the plot. The coordinates of the plot centers were measured using one of two methods: 1) using a Topcon GR-3 RTK rover and Topcon GB-3 RTK base station observing the pseudo-range and carrier phase of both GPS and GLONASS, or 2) by averaging multiple measurements by a hand-held GNSS receiver. The two methods were used on 57% and 43% of the plots in the current study, respectively.

A full five-year cycle of NFI data (2013–2017) was utilized. The total number of forested NFI plots in the study area ($n=$ 8431) was reduced to include only plots covered by the ArcticDEM data and with ArcticCHM (see section 2.4) mean height in the range of −10 m to 30 m, corresponding to the fourth and 97th percentiles, respectively (Fig. 1). These thresholds were deemed necessary to remove the occurrence of sparse high or low height values while avoiding to discard a large portion of the NFI plots with ArcticCHM mean height < 0 m (Fig. 1).

Overall, a total of $n=$ 7710 NFI plots or 91.5% of the total number of plots in the study area were available for modeling. The comparison of the summary statistics for AGB according to the original and subset datasets reported in Table 1 reveal that the sub-setting did not affect the distribution of the AGB markedly.

2.3. DTM

A freely available national-level DTM of 10 m resolution (DTM10) was used to normalize the ArcticDEM (section 2.4) to the height above ground (ArcticCHM). The DTM10 product from the Norwegian Mapping Authority (Kartverket, 2019) was generated using a combination of airborne photogrammetric data and ALS data. The ALS data have been acquired over the past ten years as part of a National effort in producing a high-resolution DTM for the whole of Norway. Approximately 70% of the DTM in the study area was generated using ALS data.

The DTM10 heights were converted from the orthometric national vertical datum NN2000 to the ellipsoidal vertical datum WGS84, in order to fit the vertical datum of the ArcticDEM.

2.4. ArcticDEM and ArcticCHM

ArcticDEM (Porter et al., 2018) is a public-private initiative, including the National Science Foundation (NSF) and The National Geospatial-Intelligence Agency (NGA). The initiative aimed to produce high resolution (2 m × 2 m pixels) DSMs for the global land area north of 60°. ArcticDEM data were freely available and generated by photogrammetric processing of in-track and cross-track image stereo pairs from the ©DigitalGlobe, Inc. constellation (i.e., WorldView 1, 2, and 3). The photogrammetric processing was performed by the "Surface Extraction with TIN-based Search-space Minimization" (SETSM) algorithm (Noh and Howat, 2015). The data are published in two main formats: i) time-stamped strips corresponding to single stereo pair image swaths and ii) a seamless mosaic of 50 × 50 km tiles which has been compiled from multiple strips that have been mosaicked by co-registration using Geoscience Laser Altimeter System (GLAS) data, blending and feathering to reduce edge-matching artefact. In this study, we used the mosaicked version since it represents the most readily usable data source. It is however important to note that despite being a mosaic, these data are characterized by voids due to cloud-cover or steep terrain and by the presence of some artefact (e.g., edges between neighboring swaths acquired in different seasons). While efforts have been made to include only the best-available imagery in the final mosaicked product, it is important to recognize that the ArcticDEM mosaic has been assembled from imagery collected over several years and includes data collected throughout all seasons.

We used 231 ArcticDEM mosaics 50 × 50 km tiles from release no.7 with a total size of 398 GB. Despite the ArcticDEM mosaic lacked metadata on acquisition dates, it is relevant to mention that most of the HRSI acquisitions available over Norway were performed during the period 2013–2015 and during 2017. The majority of scenes for the study domain were acquired between March and August.

We normalized the height data, i.e., converted from the elevation above the ellipsoid to height above-ground values by subtracting the DTM10 corresponding to each pixel. The result of the normalization is often referred to as a CHM and within this study will be referred to as ArcticCHM. For each NFI plot we extracted four explanatory variables from the ArcticCHM data: mean, standard deviation (sd), 20th (p20), and 90th (p90) percentiles of the height values of all pixels with centers within the plot area. Fig. 2 shows the location of Norway with respect to the entire archive of ArcticDEM data, the NFI plot distribution across Norway, and the available ArcticDEM data.

2.5. Sentinel-2

A wall-to-wall Sentinel-2 level-2A cloud-free mosaic was produced for the entirety of Norway using scenes acquired between June 30th and July 31st, 2018 and contained the bands 2 through 8, 8A, 11, and 12. The mosaic was created by the following steps: for each downloaded Sentinel-2 scene, we created a single PCI Geomatics file containing the aforementioned bands. Bands with 20 m resolution were resampled to 10 m with nearest neighbor resampling. Then within each scene, polygons were manually drawn over clouds and cloud-shadows and replaced with cloudless scenes.

The mosaicking was done in the PCI Geomatics Mosaic Tool and was first done scene-by-scene, followed by mosaicking several scenes with equal UTM zones to one larger block. All of the cloud-free blocks were then re-projected to the ETRS89 UTM Zone 33 N with cubic convolution

Table 1
Summary statistics for above-ground biomass (t ha^{-1}) for the original and subset NFI data.

	Min	Maximum	Mean	Median	Standard deviation	Mean absolute deviation
All plots (n = 8431)	0.1	825.4	57.2	36.6	64.0	43.5
Selected plots (n = 7710)	0.1	825.4	56.7	36.5	63.5	43.5

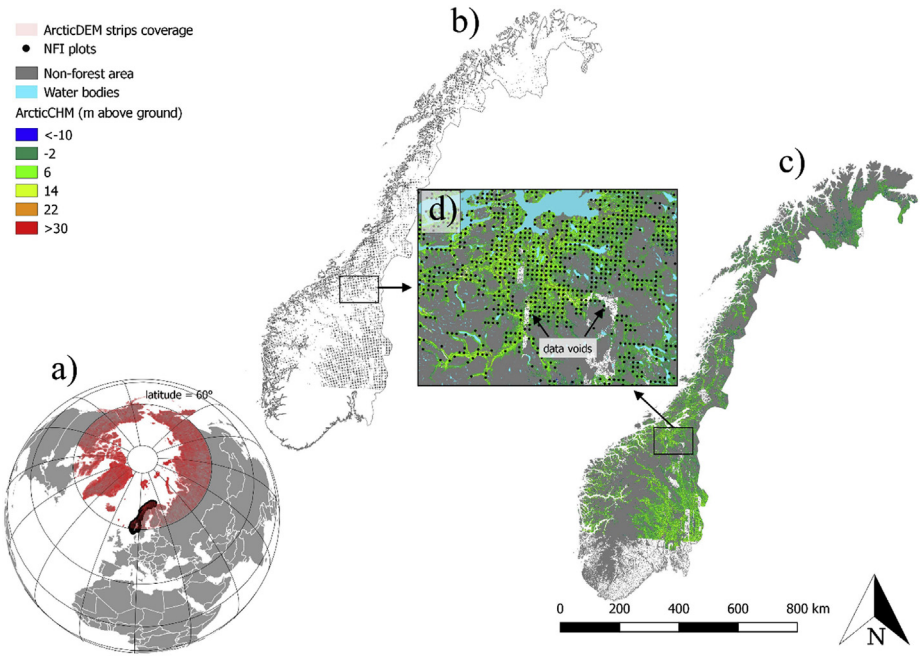

Fig. 2. Overview of: a) the study area location with coverage of ArcticDEM strip data (in red), b) the distribution of the national forest inventory plots available for this study, c) the coverage of ArcticCHM data over the forest area, and d) detail on a smaller area (including data voids). (For interpretation of the references to color in this figure legend, the reader is referred to the Web version of this article.)

resampling, and finally mosaicked together to one large file. In order to derive a seamless mosaic, dodging-points were used for color balancing, including contrast and brightness adjustment. All dodging-points were distributed on the cutline between two scenes and statistics were calculated in a search area of 64 × 64 pixels on all bands.

Explanatory variables were derived by overlaying the mosaic with the sample plots and extracting the area-weighted means of the pixels intersecting with the sample plot polygons.

2.6. Statistical methods

Our statistical modelling approach can be summarized in three steps: 1) fitting a random forest model predicting AGB; 2) validating the model at the plot level through a k-fold cross-validation; and 3) assessing the effect of forest- and terrain-specific factors (i.e., tree species, tree density, forest productivity, slope, aspect, and topographical position index) on the model residuals. These three steps were performed for three sets of explanatory variables, namely: ArcticCHM data, Sentinel-2 data (S2), and a combination of the two (ArcticCHM + S2). Furthermore, the latitude and longitude were also used as explanatory variables for all the models.

2.7. Model fitting

Random forest (Breiman, 2001) was used to model AGB. Random forest is an ensemble regression tree method based on un-correlated decision trees (Immitzer et al., 2016). The random forest algorithm was selected after preliminary analysis showed that it had better performance over multiple linear regression models. One of the advantages of random forest is that it allows using efficiently high-dimensional and correlated data while minimizing the risk of overfitting (Breiman, 2001, 2002).

The variable importance in terms of node purity (i.e., a measure related to the loss function relying on the mean square error and based on which best splits are chosen) was compared between the different models.

2.8. Model validation

We validated the models at plot level using k-fold cross-validation (CV), where the folds were defined by the plots included within each ArcticDEM mosaic tile. The CV was an iterative procedure where the number of iterations was set equal to the total number of ArcticDEM mosaic tiles. The average number of plots per tile was 47, with a minimum of one and a maximum of 178. The cross-validated predictions were then used to compute the root mean square error (RMSE), mean difference (MD), and their respective values as the percentage of the mean AGB ($RMSE_{\%}$ and $MD_{\%}$). The RMSE and MD were calculated as

$$\mathrm{RMSE} = \sqrt{\frac{\sum_{i=1}^{n} (y_i - \hat{y}_i)^2}{n}} \quad \text{Eq. 1}$$

and

$$\mathrm{MD} = \frac{\sum_{i=1}^{n} y_i - \hat{y}_i}{n} \quad \text{Eq. 2}$$

where $i = 1,\ldots,n$ and $n = 7710 =$ number of plots, y_i is plot-level AGB and $\hat{y}_i$ is the predicted AGB after cross-validation.

2.9. Assessing the effect of the forest- and terrain-specific factors.

Residual analysis was performed to understand which forest- and terrain-specific factors were most influential on the AGB models' predictive accuracy. Factors such as tree species, tree density, forest productivity, slope, aspect, and topographical position index are known to affect the quality of HRSI DEMs. For each of these factors, we assessed the boxplots of the residuals categorized either by class (i.e., tree species) or by ten percentile intervals (i.e., 10th, 20th, 30th,…,100th percentiles). Furthermore, we assessed whether the residuals were characterized by a geographical component (i.e., presence of regional biases) by visually assessing maps of the residuals aggregated into 50 km × 50 km grid cell mean values.

To gain further insights into the predictive ability of ArcticCHM, S2, and ArcticCHM + S2 models, we predicted AGB for the area corresponding to a single ArcticDEM tile and compared the prediction maps visually. We subjectively selected an area that included different ArcticCHM data quality scenarios, including areas with 1) data voids; 2) artifacts due to adjacent acquisitions performed under different seasons (i.e., summer versus winter); and 3) areas with reliable and complete ArcticCHM.

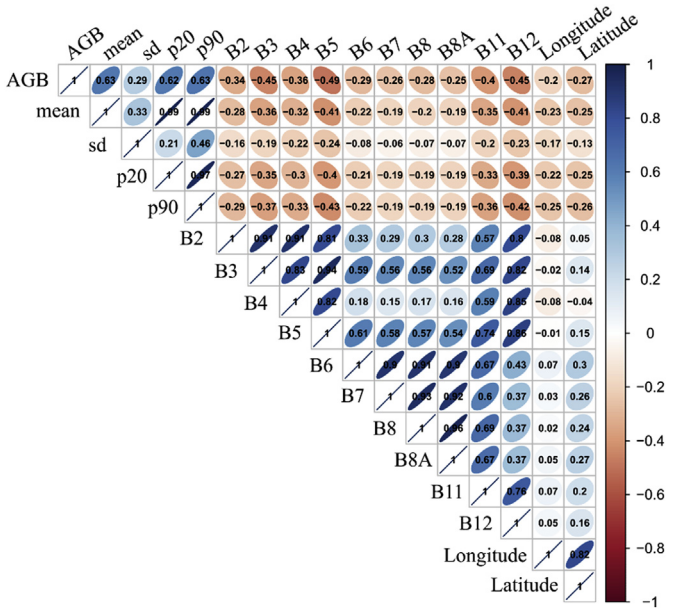

Fig. 3. Correlation matrix for the studied response (AGB; $m^3\ ha^{-1}$) and predictor variables. The direction on the major axis of the ellipse indicates whether there is a positive or negative correlation, while the colors represent the strength of the Pearson's correlation coefficient between each pair of variables. The Sentinel-2 bands are denoted as B2, B3, …, B12. (For interpretation of the references to color in this figure legend, the reader is referred to the Web version of this article.)

Furthermore, to better understand the errors in the ArcticCHM, we performed assessed it over treeless areas, where the ArcticDEM should correspond to the DTM10. Such an analysis can provide useful information on the driving sources of uncertainty in the ArcticCHM data. We selected a systematic sample of points at the intersection of a 1 km × 1 km grid over the entire study area and located in treeless areas. A land-use map from the Norwegian Mapping Authorities was used to exclude points in forest or urban areas (Ahlstrøm et al., 2014). For each of these points we extracted the corresponding height values from the ArcticCHM. These values were then used to analytically assess the presence of overall bias and visually detect regional biases.

Table 2
Summary diagnostics for the AGB models including the percentage of the variance explained (% var) by the model, root mean square error (RMSE), mean difference (MD), and their values as the percentage of the mean.

	% var	RMSE ($t\ ha^{-1}$)	RMSE (%)	MD ($t\ ha^{-1}$)	MD (%)
ArcticCHM	43	47.7	84.0	−0.9	−1.6
S2	47	45.8	80.7	−1.6	−2.8
ArcticCHM + S2	57	41.4	72.8	−1.4	−2.5

3. Results

3.1. Modelling

The correlation matrix of all the variables (Fig. 3) highlights the two groups of variables derived either from ArcticCHM or Sentinel-2. The former was characterized by a Pearson's correlation coefficient with AGB in the range 0.3–0.6 while all of the Sentinel-2 bands were negatively correlated with AGB (−0.2 – -0.5 Pearson's correlation coefficient). Latitude had a slightly stronger correlation (−0.3) with AGB than longitude (−0.2).

The most important variables, according to the importance estimated by random forest, were those associated with ArcticCHM data rather than S2 (see Fig. 4). More specifically, 90th percentile (p90), and the mean were the three most important variables both for the ArcticCHM model and the ArcticCHM + S2 model. In S2 models, the variable importance decreased more gradually than for the ArcticCHM models. The three most important S2 variables were the mean of the bands 5 (red edge), 11 (short wave infra-red), and 3 (green). The longitude and latitude were among the ten most important variables for all models.

The results of the k-fold cross-validation (CV) for the models (see Table 2) revealed that the best model fit (explained variance = 0.57) and corresponding smallest RMSE ($41.4\ t\ ha^{-1}$) were found for the model using a combination of ArcticCHM and S2 explanatory variables. The S2 model predictions were slightly more accurate than the ArcticCHM model.

However, it is essential to note that for the Sentinel-2 model, we observed a saturation effect – all AGB values larger than approximately $250\ t\ ha^{-1}$ were under-predicted (see Fig. 5, top center pane). This issue was reduced when using ArcticCHM data, for which the saturation threshold was nearly twice as big as for the Sentinel-2 model (i.e., approx. $400\ t\ ha^{-1}$). However, given the vast amount of forest in Norway with low biomass density, this saturation effect is not apparent in the model fit statistics (Table 2) when comparing the S2 and ArcticCHM models. For all of the three models, the mean differences were in the

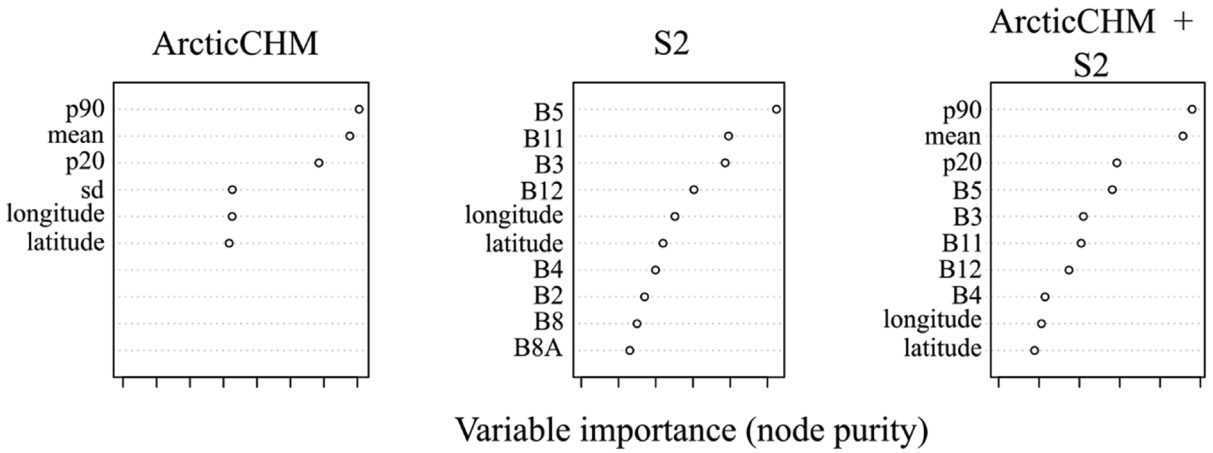

Fig. 4. Variable importance according to the node purity estimates using the random forest algorithm for the models including ArcticCHM (left pane), Sentinel-2 (center pane), and a combination of the two (right pane).

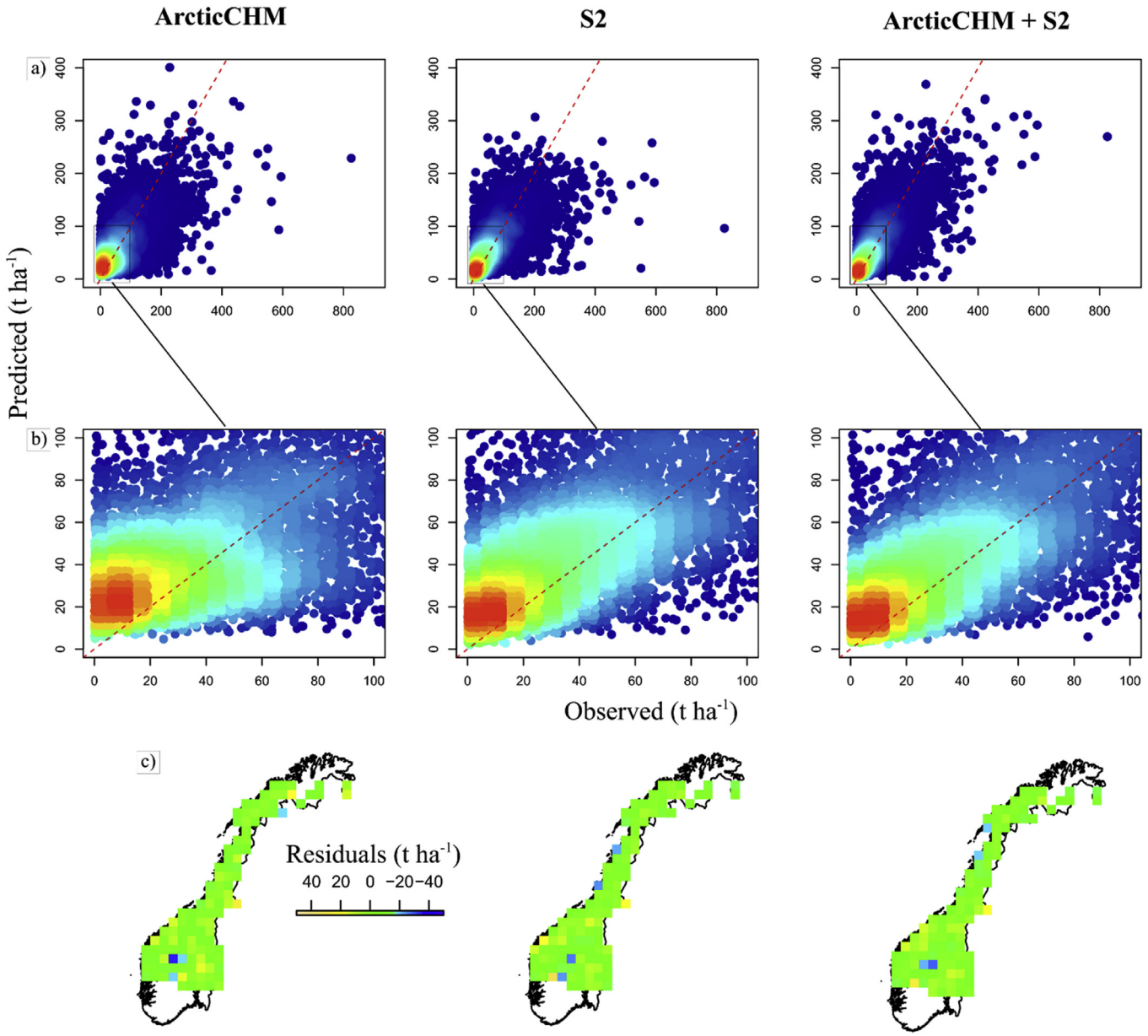

Fig. 5. Scatterplots of the observed values versus the predicted values (a), with a detail in the region between 0 and 100 t ha^{-1} (b), and residual maps over Norway aggregated in pixels of dimensions 50 km × 50 km (c) for the three models.

range −1.6 – -0.9 t ha^{-1} and were significantly different from zero (p-value of t-test < 0.05) indicating a small negative bias. We found that the combination of ArcticCHM and S2 variables led to decreasing the saturation effects of S2 and improving the model's predictive ability.

The maps of the residuals aggregated for pixels of 50 km × 50 km (see Fig. 5) indicated that for most of the country, the residuals had an average around zero. However, there were some areas characterized by a local bias which was mostly negative, meaning that the models over-predicted AGB. In particular, we observed the over-prediction of AGB in mountain areas, characterized by non-productive forests and smaller sampling intensity. On the contrary, we observed a small trend of AGB under-prediction in the south-eastern portions of the study area, characterized by spruce dominated productive forests. The combination of ArcticCHM and S2 led to a slight reduction of the systematic regional biases compared to separate models for ArcticCHM and S2 data alone.

We carried out the analyses of the effect of the forest- and terrain-specific factors on the model residuals for the ArcticCHM + S2 model alternative since it yields the most promising results (Fig. 6). The residual variance was largest for spruce dominated plots and smallest for deciduous dominated plots. However, spruce forests also have the largest AGB, and this may be the reason for the larger residual variance. The residual variance also increased with the number of trees and the AGB was in general larger than field measurements for plots with < 1000 trees ha^{-1} and smaller than those for plots with > 1400 trees ha^{-1}. Furthermore, even though the uncertainty was larger for productive forests than for non-productive forest, model predictions for the latter were more systematically larger than field measurements. The more substantial residual variance for productive forest can be partially explained by the large proportion of these plots (70% of the total) and with larger AGB values.

Amongst the terrain-specific factors, we assessed the slope, aspect, and topographical position index. The residual variance increased with the slope and when moving from flat areas or in areas with a constant slope towards ridges or valleys. On the contrary, the residual variance was rather stable across different aspect classes. Furthermore, the analysis revealed that for slopes > 30%, the systematic trend of model

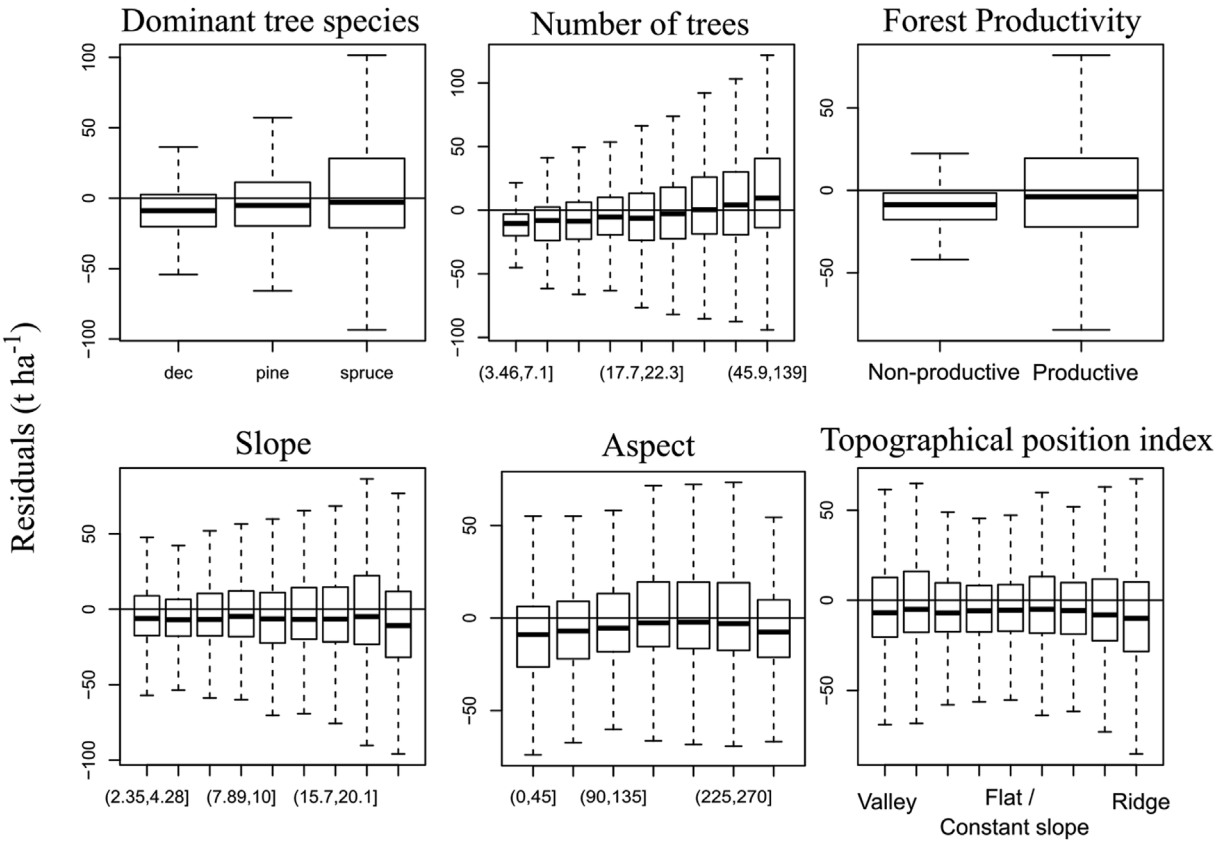

Fig. 6. Boxplots of the ArcticCHM + S2 model AGB residuals categorized according to the forest- (top row) and terrain-specific (bottom row) factors that were affecting the residuals.

predictions being larger than field measurements increased markedly. Interestingly, the trend in the residuals was minimal for south-facing slopes and gradually increased when moving towards north facing slopes. A potential explanation for the increased uncertainty of the stereogrammetric DEM in the northern slope may relate to the increased amount of shadowed regions (areas of reduced image dynamic range) such as terrain shadows.

The visual assessment of the AGB prediction for the three models (Fig. 7) was performed for two sub-areas of the selected ArcticDEM tile characterized by varying degrees of reliability of the ArcticCHM data. Fig. 7a shows an artefact visible as a north-south oriented stripe where most ArcticCHM values are negative, and no forest canopy is visible. The visual assessment confirmed the ArcticCHM + S2 model to be the one producing the most realistic predictions. In particular, the ArcticCHM + S2 model reduced the impact of artifacts (the left half of Fig. 7a) in the ArcticCHM data while reducing the under-prediction of large AGB observed for the S2 model (Fig. 7b). Further, the predictions of the ArcticCHM + S2 model were less noisy, and forest stand borders were more clearly delineated than when using Sentinel-2 data alone (Fig. 7b).

Despite the presence of local variability in the DTM quality, the median difference over entire Norway was limited to −0.2 m (Fig. 9) and, as can be seen from see Table 3, was more pronounced for areas without ALS coverage (median = −0.5 m) compared to areas with ALS coverage (median = 0.1 m).

Because of the terrain model effect, we tested the performance of the ArcticCHM and ArcticCHM + S2 models when stratifying the models according to the availability of ALS data. The RMSEs of the combination of the two models' predictions slightly decreased (47.3 t ha^{-1} and 41.0 t ha^{-1} for ArcticCHM and ArcticCHM + S2 models, respectively) compared to the values reported for the non-stratified models (47.7 t ha^{-1} and 41.4 t ha^{-1}) but the small magnitude of this improvement did not justify the use of the stratified models.

4. Discussion

The objective of this study was to assess the potential of ArcticDEM data for modelling and mapping of AGB over vast boreal forest regions. The main novelty of this study lies in the broad geographical scale at which this study was conducted (260 000 km^2) compared to previous studies (9–700 km^2) and in the availability of an extensive number of ground reference observations (n = 7710) for model calibration and validation. These two points enabled us to assess a large variety of forest types under varying topography and along a broad latitudinal gradient.

The model fit (explained variance: 0.45–0.58) and predictive accuracy in absolute terms (RMSE: 40.6–46.2 t ha^{-1}) were consistent with previous research using HRSI stereogrammetric data (explained variance: 0.43–0.79; RMSE: 31.8–70.6 t ha^{-1}) (St-Onge et al., 2008; Persson et al., 2013; Kattenborn et al., 2015; Persson, 2016; Fassnacht et al., 2017; Vastaranta et al., 2018). The comparison with alternative remotely sensed data sources to map AGB in Scandinavian forests, revealed that the plot-level RMSEs found in this study were smaller than what previously found by Fazakas et al. (1999) when using Swedish NFI and Landsat data (RMSE: 61.4 t ha^{-1}) and even smaller than using Tandem-X data (42.6–58.9 t ha^{-1}) (Næsset et al., 2011; Solberg et al., 2013). The consistency with previous research using HRSI DSMs to model AGB and performance compared to alternative data sources is encouraging for further use of ArcticDEM for larger areas and regions. This is particularly true in light of the poorer quality of these data compared to the HRSI DSMs used in small-scale detailed studies. The reduced accuracy of ArcticDEM compared to on-demand acquisitions was mostly caused by the inclusion of multiple acquisitions from different seasons causing inconsistencies or artifacts in the data. In this

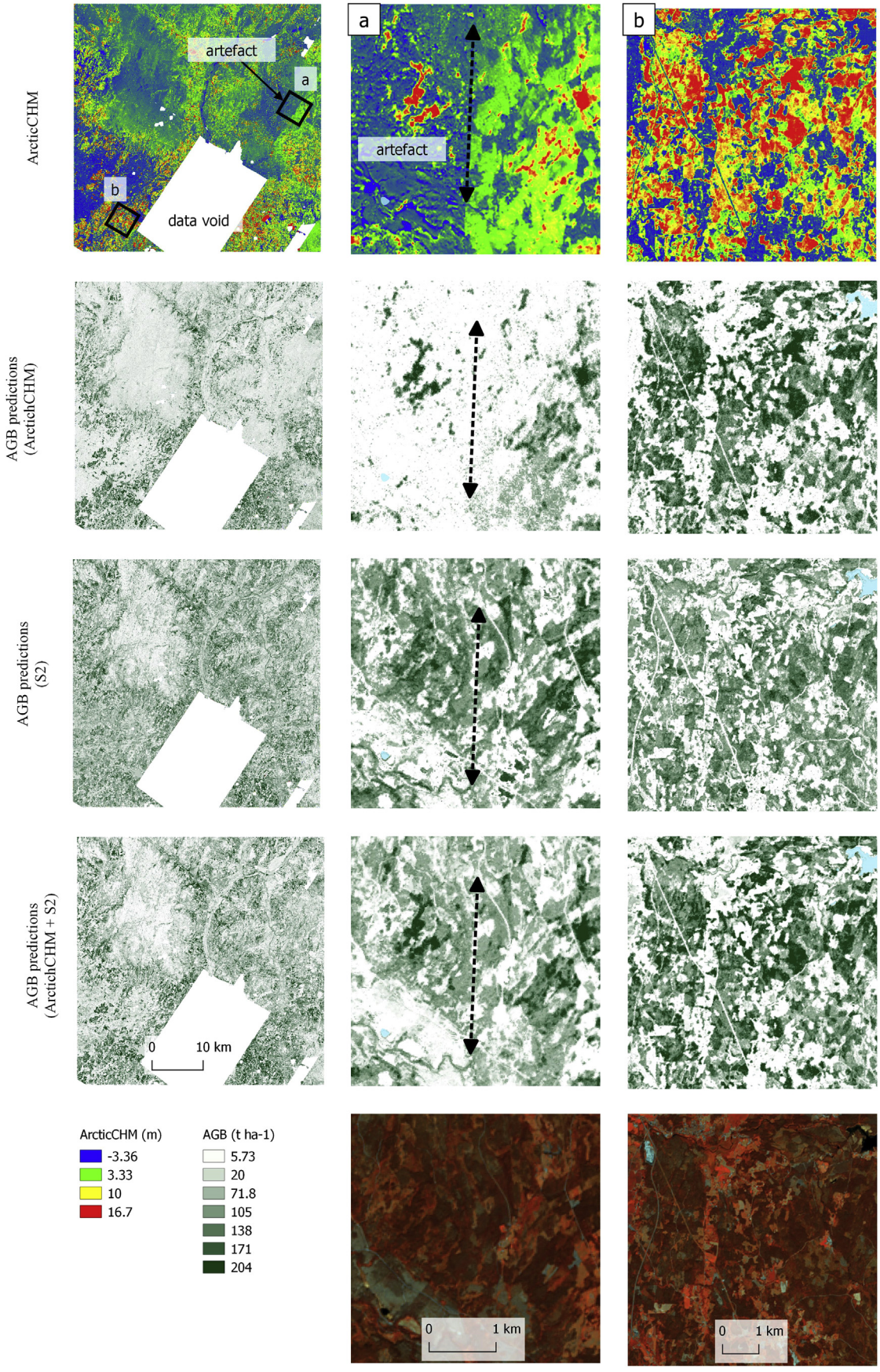

(caption on next page)

Fig. 7. Maps of AGB predicted using the three different models using either ArcticCHM, Sentinel-2, or a combination of the two (center coordinates: 60° 58′ N, 11° 27′ E). The first column represents the extent of the selected ArcticCHM tile, while the following two columns represent two details for areas where the ArcticCHM is either un-reliable (a) or of high quality (b). In (a) an artefact in the form of a north-south oriented striping corresponding to two different acquisitions done either in the summer (left side of dashed line) or the winter (right side of dashed line). In the last row, the Sentinel-2 mosaic is displayed for areas a and b to highlight the forested areas. The analysis of the ArcticCHM over treeless areas revealed a higher variability in areas where the DTM10 was not based on ALS data (Fig. 8).

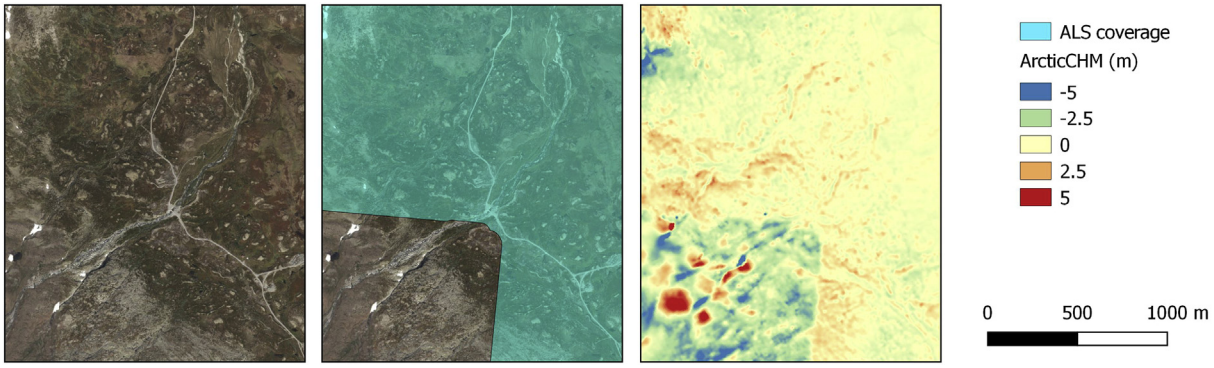

Fig. 8. ArcticCHM values in mountain areas with no tree cover and with varying quality of the DTM depending on ALS coverage.

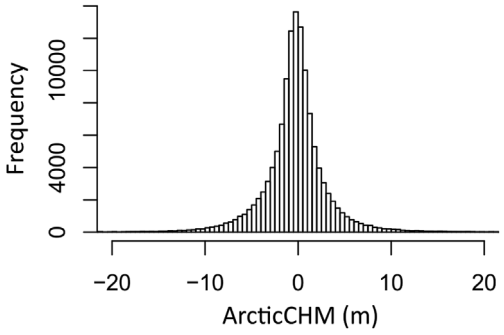

Fig. 9. Histogram of the ArcticCHM values in treeless areas based on the sample of points selected over the entire study area. The range in x-axis was reduced to ArcticCHM values < -20 m and > 20 m for visualization purposes.

Table 3
The median difference between ArcticDEM and DTM10 over treeless areas (n = 127 079 points) subdivided into areas with ALS DTM or not.

ALS DTM	Median of difference (m)
Yes (42%)	0.1
No (58%)	−0.5

respect, the sun angle has previously been determined as one of the most important factors affecting the features captured in HRSI DSMs (Montesano et al. 2017, 2019). Montesano et al. (2017, 2019) indicate that HRSI DSMs will capture different surfaces depending on an acquisition's sun elevation angle, and this will affect the estimates of the vertical position of forest canopies above the ground. Montesano et al. (2019) also highlighted the negative effect of snow-cover on the quality of some canopy surface estimates from HRSI DSMs. Within the ArcticDEM acquisitions over Norway, a total of 589 out of 3133 acquisitions (18%) were performed between December 1st and April 1st when much of the country is covered in snow, and the sun angle is low. The presence of snow- or cloud-cover in the HRSI acquisition used in the ArcticDEM, caused the presence of data voids in the ArcticDEM data.

In contrast to most previous studies, which used HRSI DEMs co-registered using locally available ALS data, the ArcticDEM data were co-registered using sparse GLAS data. While GLAS data represent the best currently available open-data source covering the entire boreal zone, the inherent errors are likely to be larger than what was previously reported for HRSI DEMs (Montesano et al. 2017, 2019; Piermattei et al., 2018). In the near future, the availability of space-borne data from ICESat-2 (Neuenschwander and Pitts, 2019) will enable to obtain denser networks of ground control points for co-registration purposes, thus potentially offering increased accuracy of HRSI DEMs. The analysis of the difference between ArcticDEM and DTM10 (i.e., the ArcticCHM) over treeless areas showed no alarming systematic shift between the two surfaces. We identified the quality of the terrain model as the main driver of systematic and random errors in ArcticCHM data.

Topographic complexity was a factor in our study, and our findings confirm the results by Piermattei et al. (2018) indicating an increase in uncertainty of HRSI DEMs with terrain slope. In line with these results, the analysis of the topographic position on the AGB residuals revealed that the smallest uncertainty was found for areas characterized by a constant slope (i.e., flat areas or areas on a slope). This study also showed systematic errors in predictions from the ArcticCHM + S2 model given aspect; where systematic errors were smallest on southern facing slopes and largest on northern facing slopes. Such systematic errors may be explained by the fact that both ArctiCHM and S2 were derived from optical data and their quality was reduced on north-facing slopes due to topographic shading.

In this study, we combined ArcticCHM with Sentinel-2 data as a means to improve a model's fit and predictive accuracy. We adopted this approach to provide a new understanding of the synergies between two freely available datasets for the entire boreal zone. The results highlight the importance of the synergy between 3D and multispectral information for AGB modelling. This study found that Sentinel-2 data alone yielded relatively accurate models. For S2 models the model fit (explained variance = 0.47) was of similar magnitude to what was previously found (explained variance = 0.48) in a sub-area of the current study area for growing stock volume by Puliti et al. (2018). Our results are encouraging for further use of Sentinel-2 for AGB mapping in boreal forests. A noteworthy finding of this study was the S2 model explained more variation and had a smaller RMSE than Arctic CHM variables. A possible explanation may lie in the fact that the ArcticCHM includes a large HRSI acquisition variability (atmospheric, seasonal and sun-target-sensor geometry) while the Sentinel-2 mosaic was generated using images acquired within two summer months and was normalized for edge effects, thus limiting the variation within the dataset. The importance of the consistency of the multispectral data had been previously highlighted by Næsset et al. (2016), who found that single-date RapidEye data outperformed TanDEM-X data in the estimation of AGB

but that this performance declined considerably when using more heterogeneous data.

The negative effects of a larger acquisition variability resulted in 20% of the field plots where the 90th percentile of the ArcticCHM was negative. These negative values were mostly found in areas where the ArcticCHM was of poor quality and did not detect canopy height (see artefact in Fig. 7a). Given such characteristics, these areas could be excluded from the ArcticCHM data as considered similar to void areas. However, in this study we did not discard the NFI plots with negative ArcticCHM values in order to assess the full ArcticDEM mosaic product. When using only the ArcticCHM, the presence of the negative heights resulted in a severe under prediction of AGB (see ArcticCHM predictions within the artefact in Fig. 7a). Interestingly, when combining ArcticCHM with Sentinel-2, we were able to substantially reduce such errors (see ArcticCHM + S2 predictions within the artefact in Fig. 7a). These results demonstrate the utility of augmenting highly variable ArcticCHM data with a wall-to-wall layer of Sentinel-2 data. Such synergy allowed the model to predict realistic AGB values even in areas where ArcticCHM was unreliable (see ArcticCHM + S2 predictions in Fig. 7b).

Similarly to areas with negative values, data voids (i.e., because of lack of coverage, snow- or cloud-cover) represent a considerable limitation to the use of ArcticDEM for large-scale mapping purposes. Even though the extent of the data voids was limited within this study (8.5% of the forest area), large portions of the hemiboreal are characterized by voids in the ArcticDEM data (e.g., Siberia). Similarly to areas with negative values, data voids could be filled by relying on the synergy with Sentinel-2 data, thus allowing producing an AGB wall-to-wall product. Future studies should investigate the possibility to use space-borne multispectral imagery for filling gaps in HRSI stereogrammetric data in a similar fashion to what has been done in the ArcticCHM + S2 model.

In this study, we utilized the mosaicked version of the ArcticDEM data which lacks details on HRSI acquisition characteristics (e.g., time and date) and which limited the possibility to investigate the effect of seasonal variations in the quality of the ArcticDEM. Further work with the ArcticDEM should consider the stripped version, which by including the timestamp can potentially improve the modelling by for example chronologically matching the NFI data corresponding to each strip, thus avoiding temporal mismatch issues between field and remotely sensed data (e.g., due to harvests). Furthermore, the possibility to subset the data based on solar geometry and seasonal effects enables a sub-setting of the highest quality DEMs, rather than using mosaicked information over multiple acquisitions.

In the context of global efforts to measure, report, and verify carbon stock changes, ArcticDEM represents the most complete and freely available 3D data covering the hemiboreal zone. However, the uncertainty of the repeatability in time of programs such as ArcticDEM limits the possibility to base long-term monitoring programs on HRSI DEMs. More appropriate use of ArcticDEM data would be to estimate and map present AGB stock across boreal forest. Such effort would provide nearly full coverage, consistent and high-resolution predictions of AGB for forest areas otherwise characterized by sparse, low resolution, and uncertain information on AGB stocks (Dong et al., 2003; Boudreau et al., 2008; Thurner et al., 2014). In addition to providing a better understanding of the current state of AGB stocks in boreal forests such product could become the benchmark for any future efforts to monitor AGB changes in boreal forests based on freely available spaceborne data such as Sentinel-2.

A unique aspect of this study was that a DTM was available for the entirety of Norway, thus allowing for the production of the ArcticCHM from the ArcticDEM. At a boreal scale, accurate DTMs are scarce, and thus alternative methods are needed to obtain canopy heights from ArcticDEM. One potential source of global DTM is the WorldDEM DTM (AIRBUS, 2019), a 12 m resolution commercial product from TanDEM-X data. An alternative approach has been proposed by Meddens et al. (2018), who predicted canopy height using a model combining HRSI multispectral and ArcticDEM data with a sample of ALS data as reference height. While these represent potential opportunities, both rely on commercial products that are not readily available to the international scientific community. Hence, future research should address the use of freely available data for mapping AGB across boreal forests. The merit of this study was to provide first best-case scenario insights (i.e., availability of DTM) into the relationships between forest AGB and ArcticCHM at a nation-wide scale. The results of this study form a benchmark for future efforts in the use of HRSI stereogrammetric data for large-scale forest AGB mapping.

5. Conclusion

To the best of our knowledge, this study represents the first attempt to utilize HRSI DEMs data to model AGB at a national scale. The main contribution of the study is the application of the large-scale NFI field dataset and its use to evaluate ArcticDEM, Sentinel-2, and their combination for AGB modeling. Based on the results of this study we conclude that 1) AGB can be estimated with similar accuracy when using ArcticCHM or Sentinel-2 data, 2) considerable synergies can be expected when combining ArcticCHM with Sentinel-2 data, 3) Both forest- and terrain-specific characteristics affect the uncertainty of predictions deriving from ArcticCHM models.

Acknowledgements

This study was funded by the Norwegian Space Centre (Norsk Romsenter) project n. JOP.01.19.2 “Use of space-borne 3D data and national forest inventory data to estimate forest biomass in Norway”. DEMs were provided by the Polar Geospatial Center under NSF-OPP awards 1043681, 1559691, and 1542736. The Sentinel-2 data were mosaicked and provided by the Norwegian Mapping Authority (Kartverket), supported by the Norwegian Space Centre project n. NIT.02.18.5. The study was further supported by NIBIO and by National Aeronautical and Space Administration's (NASA) Terrestrial Ecology Program Terrestrial Ecology Program award 16-CARBON16-0124.

References

Ahlstrøm, A., Bjørkelo, K., Frydenlund, J., 2014. AR5 klassifikasjonssystem - klassifikasjon av arealressurser (In Norwegian).
AIRBUS, 2019. WorldDEM™ technical product specification.
Boudreau, J., Nelson, R.F., Margolis, H.A., Beaudoin, A., Guindon, L., Kimes, D.S., 2008. Regional aboveground forest biomass using airborne and spaceborne LiDAR in Québec. Remote Sens. Environ. 112, 3876–3890.
Breiman, L., 2001. Random forests. Mach. Learn. 45, 5–32.
Breiman, L., 2002. Manual on Setting up, Using, and Understanding Random Forests V3. 1, vol. 1 Statistics Department University of California Berkeley, CA, USA.
Dong, J., Kaufmann, R.K., Myneni, R.B., Tucker, C.J., Kauppi, P.E., Liski, J., Buermann, W., Alexeyev, V., Hughes, M.K., 2003. Remote sensing estimates of boreal and temperate forest woody biomass: carbon pools, sources, and sinks. Remote Sens. Environ. 84, 393–410.
Fassnacht, F.E., Mangold, D., Schäfer, J., Immitzer, M., Kattenborn, T., Koch, B., Latifi, H., 2017. Estimating stand density, biomass and tree species from very high resolution stereo-imagery – towards an all-in-one sensor for forestry applications? Forestry: Int. J. Financ. Res. 90, 613–631.
Fazakas, Z., Nilsson, M., Olsson, H., 1999. Regional forest biomass and wood volume estimation using satellite data and ancillary data. Agric. For. Meteorol. 98–99, 417–425.
Immitzer, M., Stepper, C., Böck, S., Straub, C., Atzberger, C., 2016. Use of WorldView-2 stereo imagery and National Forest Inventory data for wall-to-wall mapping of growing stock. For. Ecol. Manag. 359, 232–246.
Kartverket, 2019. Hoydedata.no.
Kattenborn, T., Maack, J., Faßnacht, F., Enßle, F., Ermert, J., Koch, B., 2015. Mapping forest biomass from space – fusion of hyperspectral EO1-hyperion data and Tandem-X and WorldView-2 canopy height models. Int. J. Appl. Earth Obs. Geoinf. 35, 359–367.
Kuusela, K., 1990. The dynamics of boreal coniferous forests. In: Helsinki, Finland.
Marklund, L.G., 1988. Biomassafunktioner för tall, gran och björk i Sverige. In: Sveriges Landbruksuniversitet, pp. 1–73.
Meddens, A.J.H., Vierling, L.A., Eitel, J.U.H., Jennewein, J.S., White, J.C., Wulder, M.A., 2018. Developing 5 m resolution canopy height and digital terrain models from WorldView and ArcticDEM data. Remote Sens. Environ. 218, 174–188.

Montesano, P.M., Neigh, C., Sun, G., Duncanson, L., Van Den Hoek, J., Ranson, K.J., 2017. The use of sun elevation angle for stereogrammetric boreal forest height in open canopies. Remote Sens. Environ. 196, 76–88.
Montesano, P.M., Neigh, C.S.R., Wagner, W., Wooten, M., Cook, B.D., 2019. Boreal canopy surfaces from spaceborne stereogrammetry. Remote Sens. Environ. 225, 148–159.
Næsset, E., Gobakken, T., Solberg, S., Gregoire, T.G., Nelson, R., Ståhl, G., Weydahl, D., 2011. Model-assisted regional forest biomass estimation using LiDAR and InSAR as auxiliary data: a case study from a boreal forest area. Remote Sens. Environ. 115, 3599–3614.
Næsset, E., Ørka, H.O., Solberg, S., Bollandsås, O.M., Hansen, E.H., Mauya, E., Zahabu, E., Malimbwi, R., Chamuya, N., Olsson, H., Gobakken, T., 2016. Mapping and estimating forest area and aboveground biomass in miombo woodlands in Tanzania using data from airborne laser scanning, TanDEM-X, RapidEye, and global forest maps: a comparison of estimated precision. Remote Sens. Environ. 175, 282–300.
Neigh, C.S.R., Masek, J.G., Bourget, P., Rishmawi, K., Zhao, F., Huang, C., Cook, B.D., Nelson, R.F., 2016. Regional rates of young US forest growth estimated from annual Landsat disturbance history and IKONOS stereo imagery. Remote Sens. Environ. 173, 282–293.
Neuenschwander, A., Pitts, K., 2019. The ATL08 land and vegetation product for the ICESat-2 mission. Remote Sens. Environ. 221, 247–259.
NIBIO, N.I.o.B.R., 2015. Landsskogtakseringen—Norway's national forest inventory.
Noh, M.-J., Howat, I.M., 2015. Automated stereo-photogrammetric DEM generation at high latitudes: surface Extraction with TIN-based Search-space Minimization (SETSM) validation and demonstration over glaciated regions. GIScience Remote Sens. 52, 198–217.
Pan, Y., Birdsey, R.A., Fang, J., Houghton, R., Kauppi, P.E., Kurz, W.A., Phillips, O.L., Shvidenko, A., Lewis, S.L., Canadell, J.G., Ciais, P., Jackson, R.B., Pacala, S.W., McGuire, A.D., Piao, S., Rautiainen, A., Sitch, S., Hayes, D., 2011. A large and persistent carbon sink in the world's forests. Science 333, 988–993.
Pearse, G.D., Dash, J.P., Persson, H.J., Watt, M.S., 2018. Comparison of high-density LiDAR and satellite photogrammetry for forest inventory. ISPRS J. Photogrammetry Remote Sens. 142, 257–267.
Persson, H., Wallerman, J., Olsson, H., Fransson, J.E.S., 2013. Estimating forest biomass and height using optical stereo satellite data and a DTM from laser scanning data. Can. J. Remote Sens. 39, 251–262.
Persson, H.J., 2016. Estimation of boreal forest attributes from very high resolution pléiades data. Remote Sens. 8, 736.
Persson, H.J., Perko, R., 2016. Assessment of boreal forest height from WorldView-2 satellite stereo images. Remote Sens. Lett. 7, 1150–1159.
Piermattei, L., Marty, M., Karel, W., Ressl, C., Hollaus, M., Ginzler, C., Pfeifer, N., 2018. Impact of the acquisition geometry of very high-resolution pléiades imagery on the accuracy of canopy height models over forested alpine regions. Remote Sens. 10, 1542.
Poon, J., Fraser, C.S., Chunsun, Z., Li, Z., Gruen, A., 2005. Quality assessment of digital surface models generated from IKONOS imagery. Photogramm. Rec. 20, 162–171.
Porter, C., Morin, P., Howat, I., Noh, M.-J., Bates, B., Peterman, K., Keesey, S., Schlenk, M., Gardiner, J., Tomko, K., Willis, M., Kelleher, C., Cloutier, M., Husby, E., Foga, S., Nakamura, H., Platson, M., Wethington Jr., M., Williamson, C., Bauer, G., Enos, J., Arnold, G., Kramer, W., Becker, P., Doshi, A., D'Souza, C., Cummens, P., Laurier, F., Bojesen, M., 2018. ArcticDEM. In: Harvard Dataverse.
Puliti, S., Saarela, S., Gobakken, T., Ståhl, G., Næsset, E., 2018. Combining UAV and Sentinel-2 auxiliary data for forest growing stock volume estimation through hierarchical model-based inference. Remote Sens. Environ. 204, 485–497.
Solberg, S., Astrup, R., Breidenbach, J., Nilsen, B., Weydahl, D., 2013. Monitoring spruce volume and biomass with InSAR data from TanDEM-X. Remote Sens. Environ. 139, 60–67.
St-Onge, B., Hu, Y., Vega, C., 2008. Mapping the height and above-ground biomass of a mixed forest using lidar and stereo Ikonos images. Int. J. Remote Sens. 29, 1277–1294.
Straub, C., Tian, J., Seitz, R., Reinartz, P., 2013. Assessment of Cartosat-1 and WorldView-2 stereo imagery in combination with a LiDAR-DTM for timber volume estimation in a highly structured forest in Germany. Forestry: Int. J. Financ. Res. 86, 463–473.
Thurner, M., Beer, C., Santoro, M., Carvalhais, N., Wutzler, T., Schepaschenko, D., Shvidenko, A., Kompter, E., Ahrens, B., Levick, S.R., Schmullius, C., 2014. Carbon stock and density of northern boreal and temperate forests. Glob. Ecol. Biogeogr. 23, 297–310.
Tomter, S., Hylen, G., Nilsen, J.E., 2010. Norways national forest ,inventory. In: Tomppo, E., Gschwantner, T., Lawrence, M., McRoberts, R. (Eds.), National Forest Inventories: Pathways for Common Reporting. Springer, Berlin.
Vastaranta, M., Yu, X., Luoma, V., Karjalainen, M., Saarinen, N., Wulder, M.A., White, J.C., Persson, H.J., Hollaus, M., Yrttimaa, T., Holopainen, M., Hyyppä, J., 2018. Aboveground forest biomass derived using multiple dates of WorldView-2 stereo-imagery: quantifying the improvement in estimation accuracy. Int. J. Remote Sens. 39, 8766–8783.
Wallerman, J., Fransson, J.E.S., Bohlin, J., Reese, H., Olsson, H., 2010. Forest mapping using 3D data from SPOT-5 HRS and Z/I DMC. In: 2010 IEEE International Geoscience and Remote Sensing Symposium, pp. 64–67.